Chemical Engineering Journal 288 (2016) 739–744

Contents lists available at ScienceDirect

Chemical Engineering Journal

journal homepage: www.elsevier.com/locate/cej

Remediation of arsenic(III) from aqueous solutions using improved nanoscale zero-valent iron on pumice

Tingyi Liu [a], Yilin Yang [a], Zhong-Liang Wang [a,b,*], Yanqiu Sun [a]

[a] Tianjin Key Laboratory of Water Resources and Environment, Tianjin Normal University, Tianjin 300387, China
[b] State Key Laboratory of Environmental Geochemistry, Institute of Geochemistry, Chinese Academy of Sciences, Guiyang 550002, China

HIGHLIGHTS

- NZVI supported on pumice and modified by chitosan was successfully prepared.
- The dispersion and stability of NZVI on CS-P-NZVI were obviously enhanced.
- As(III) can be quickly and effectively removed by CS-P-NZVI.
- CS-P-NZVI was an effective material for both in situ and ex situ remediation.

ARTICLE INFO

Article history:
Received 18 September 2015
Received in revised form 21 December 2015
Accepted 21 December 2015
Available online 29 December 2015

Keywords:
Nanoscale zero-valent iron
Pumice
Chitosan
Arsenic(III)
Wastewater

ABSTRACT

The removal of arsenic(III), one of the most poisonous wastewater pollutants, was investigated using nanoscale zero-valent iron supported onto pumice and modified by chitosan (CS-P-NZVI). Scanning electron microscopy (SEM) analysis revealed that NZVI was distributed dispersedly on CS-P-NZVI without being oxidized. As(III) could be removed by adsorption on CS-P-NZVI in a very short time (minute scale) with high removal rates (more than 99.5%) over a wide range of pH (2.01–12.54) and concentration (20–100 mg/L). The removal of As(III) by CS-P-NZVI agreed well with the pseudo-first-order reaction kinetics and pseudo-second-order reaction kinetics. Reaction rate constants (K_{obs}) ranged from 0.27 to 0.96 min^{-1} at varied NZVI dosage. Freundlich isotherm provided a good model of the sorption system, indicating that CS-P-NZVI was heterogeneous in the surface properties. The thermodynamic parameters suggested that As(III) adsorption by CS-P-NZVI was a spontaneous and exothermic process. X-ray photoelectron spectroscopy (XPS) and atomic fluorescence spectrophotometer (AFS) analyses indicated that As(III) was only physically adsorbed on the surface of CS-P-NZVI within 60 min. Our results indicated that CS-P-NZVI might be an effective material for both in situ and ex situ remediation.

1. Introduction

Arsenic has been used in many domains of wood preservation, pyrotechnics, pesticides and semiconductor solar cells. In the environment, arsenic usually existed in inorganic and organic forms. Inorganic arsenic, especially As_2O_3, was known to be more poisonous than organic one [1]. Arsenic exists in groundwater predominantly as inorganic arsenite(III) (H_3AsO_3, $H_2AsO_3^{1-}$ and $HAsO_3^{2-}$) [2].

However, arsenic would cause serious impacts on the cardiovascular system and even resulted in the hepatic damage at high doses [3]. Worst of all, inorganic arsenic could be easily accumulated in human tissues and combined with proteins but were not degraded gradually [4]. Hence, great attention must be required for the removal of As(III) from wastewater because of its high toxicity and mobility [5].

Due to the small size, large surface area and high reactivity, nanoscale zero-valent iron (NZVI) has exhibited great potential in a wide array of environmental remediation [6]. Varieties of pollutants, such as carbon tetrachloride, nitrates, organic compounds, heavy metals, arsenite, and so on, were effectively removed by NZVI [7,8]. However, an easy formation of oxides and agglomeration, resulting in the rapid loss in reactivity, challenged and limited the application of NZVI in environmental remediation [9]. To overcome the problems, anionic polymer [10], starches [9], chitosan [11], carboxymethyl cellulose [12] and guar gum [13] have been used to enhance stability of NZVI particles. Furthermore, pumice,

* Corresponding author at: Tianjin Key Laboratory of Water Resources and Environment, Tianjin Normal University, Tianjin 300387, China. Tel./fax: +86 22 23766256.
E-mail address: wangzhongliang@vip.skleg.cn (Z.-L. Wang).

http://dx.doi.org/10.1016/j.cej.2015.12.070
1385-8947/

bentonite and zeolite were used to increase the dispersibility NZVI particles [14–16]. To the best of our knowledge, however, few studies have focused on modifying nanoscale zero-valent iron on pumice using chitosan (CS-P-NZVI) to improve the stability and dispersibility of NZVI.

In the study, modified nanoscale zero-valent iron on pumice was tested for their ability to separate and immobilize As(III) ions from aqueous solutions. The main objectives are to: (1) characterize CS-P-NZVI and its reaction products using microscopic technology, (2) investigate the different environmental factors on As(III) remediation, (3) delineate the kinetics of As(III) adsorption, and (4) understand the removal mechanism using spectroscopic study.

2. Materials and methods

2.1. Chemicals

Iron(III) chloride hexahydrate ($FeCl_3{\cdot}6H_2O$) and sodium borohydride ($NaBH_4$) were purchased from Fuchen Chemical Reagent Manufactory (Tianjin, China). 1 g/L $AsCl_3$ solution was provided by National centre for certified reference materials (Beijing, China). Pumice with a diameter of 0.5–1.0 mm was provided by Dahe Building Materials Co. Ltd. (Hebei, China). All other chemicals were of analytical grade purity.

2.2. Preparation of CS-P-NZVI

CS-P-NZVI was prepared using conventional liquid-phase methods via the reduction of ferric ion ($FeCl_3{\cdot}6H_2O$) by borohydride ($NaBH_4$) using chitosan as a surfactant and pumice as a support material [6,11,14]. P-NZVI was successfully prepared using the previously reported procedure [14]. The fresh prepared P-NZVI was introduced into the very dilute chitosan solution (0.01 g/L) with constant stirring for 3 h. The synthesized materials were separated from the liquid solution via the magnet and washed using deionized water. CS-P-NZVI was stored in brown and sealed bottles for further use. The whole process was carried out in a nitrogen atmosphere.

2.3. Batch experiments

Effects of different experimental conditions on the removal efficiency and kinetics of As(III) were studied as the following procedure. CS-P-NZVI was added into the prepared wastewater at room temperature with mechanical agitation for 1 h. Then, the wastewater was withdrawn every 10 min using a 10 mL dispensable syringe and filtered through a 0.22 μm filter for further analysis. All experiments were performed in duplicate.

2.4. Kinetics and thermodynamic o f Hg (II) and Cr (VI) removal by P-NZVI

The effect of pH value and NZVI dosages on the reduction kinetics of As(III) was studied in accordance with a previously reported procedure [14]. An expression of the pseudo-second-order rate based on the solid capacity has been presented for the kinetics of sorption [17]

$$\frac{t}{q_t} = \frac{1}{kq_e^2} + \frac{1}{q_e}t \quad (1)$$

where k is the pseudo-second-order rate constant (g/mg min), q_e is the amount of As(III) adsorbed at equilibrium (mg/g), and q_t is amount of As(III) on the surface of CS-P-NZVI at any time t (mg/g).

The thermodynamic parameters such as enthalpy change (ΔH^0), Gibbs free energy change (ΔG^0) and entropy change (ΔS^0) were employed to evaluate the feasibility and nature of adsorption process with a previously reported procedure, as also as Langmuir and Freundlich adsorption isotherm parameters [18].

2.5. Characterization and analytical methods

The concentrations of arsenic were measured using inductively coupled plasma-mass spectrometry (ICP-MS, Elan-9000, PE). The valence of arsenic after reacting with CS-P-NZVI was analyzed using atomic fluorescence spectrophotometer (LC-AFS9780, Beijing Haiguang Instrument Co., Ltd., China). The morphological analysis of CS-P-NZVI was performed using a scanning electron microscope (SEM) (SEM, FEI Nova NanoSEM 230). The specific surface area (S_{BET}) of P-NZVI was measured with Brunauer–Emmett–Teller (BET) N_2 method. The morphological analysis of NZVI was performed using a transmission electron microscope (TEM, FEI Tecnai G2 F20). CS-P-NZVI was used to the X-ray photoelectron spectroscope (XPS, PHI 5000 Versa Probe) analysis before and after reacting with As(III), respectively.

3. Results and discussion

3.1. SEM and TEM characterization

The morphology of CS-P-NZVI and NZVI were shown in Fig. 1. It can be seen (Fig. 1(a)) that NZVI was slightly agglomerated on the surface of P-NZVI. However, NZVI was uniformly distributed on the surface of CS-P-NZVI (Fig. 1(b)) after being modified by CS. A chain-like and aggregated structure was formed because of its natural magnetism and NZVI was also covered by the passivator on the surface (Fig. 1(c)), which was also observed in other study [19]. The coverage of NZVI with CS provided enhanced resistance against the particle aggregation through the electrostatic repulsion and steric hindrance [20]. CS-P-NZVI with a 6.8% NZVI mass fraction had a S_{BET} of 38.2 m^2/g. Furthermore, NZVI particles were nearly spherical in shape and uniform in size with a mean diameter of 23.6 nm (Fig. 1(d)). As a result, NZVI was distributed dispersedly on the surface of CS-P-NZVI (Fig. 1(d)). Due to the fact that incorporating of amino groups on the chitosan to iron nanoparticles could enhance the stability of the nanoparticles [11], NZVI on CS-P-NZVI was better protected by chitosan and the oxidation was hindered. The similar phenomenon was also observed in other NZVI system [21]. Sterically hindered substrates enjoyed a broad scope and wide functional group tolerance [22]. Sterically hindered effect was the main driving force which hindered the oxidation and aggregation of NZVI [23]. Faster reaction rates have now been achieved with sterically hindered chelating alkyl phosphine ligands [24].

3.2. Kinetic of As(III) removal by CS-P-NZVI

The effect of pH (2.01–12.54) on the adsorption of As(III) (40 mg/L) on CS-P-NZVI was conducted (Fig. 2 and inset). It could be seen that K_{obs} of As(III) decreased with an increase in the initial pH and the removal rates were all more than 99.5% in the pH range of 2.01–12.54 (Fig. 2(a) and inset). However, the removal rates were little different below pH 8.49 and slightly decreased above 8.49. The phenomena could be explained by ionization of both the adsorbent and the adsorbate. When the pH was below pH 9.2 and above 9.2, H_3AsO_3 and $H_2AsO_3^-$ were the predominant species, respectively [8]. The results of the zeta potential of CS-P-NZVI showed that CS-P-NZVI was positively charged at pH < 7.6 (Fig. 3). With an increasing pH, the surface of CS-P-NZVI became dominantly negatively charged (Fig. 3), leading to the repulsion force between CS-P-NZVI and $H_2AsO_3^-$ [25]. The similar trend in

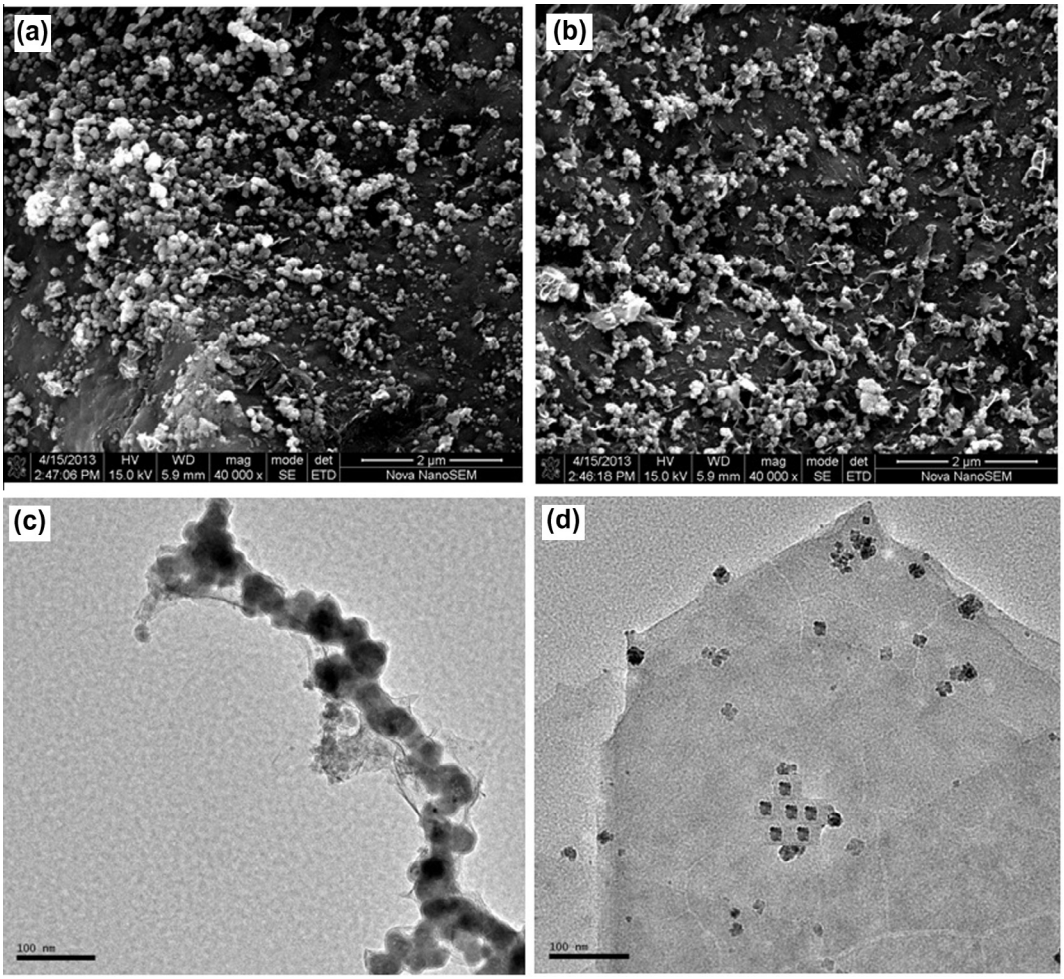

Fig. 1. The morphology of CS-P-NZVI and NZVI were analyzed: (a) SEM image of P-NZVI, (b) SEM of CS-P-NZVI, (c) TEM image of P-NZVI and (d) TEM image of CS-P-NZVI.

As(III) removal has been observed using goethite [26]. Furthermore, because of forming inner-sphere surface composites on ZVI [27], the removal rate of As(III) decreased sharply above 10 [8]. However, the surface of CS-P-NZVI was so complex that pH did not play an obvious effect on the removal rate, indicating that the high removal rate of As(III) by CS-P-NZVI might not be limited in the particular pH range.

Obviously, K_{obs} of all heavy metals displayed a good linearity to pH values with correlation coefficients (R^2) more than 0.98. This indicated that the removal of As(III) by CS-P-NZVI agreed well with the pseudo-first-order reaction kinetics. The similar phenomena had also been found in other systems using nanoscale iron, a-Fe_2O_3 nanoparticles and nanoscale iron supported on chitosan beads [21,25]. Furthermore, it could be seen from Fig. 2(b) that R^2 more than 0.99 indicated that there was strong positive evidence that As(III) sorption onto CS-P-NZVI followed the pseudo-second-order kinetic expression. However, these trend lines at different pH values were nearly identical, which meant that the nature of adsorption of As(III) on CS-P-NZVI was same. Comparing the pseudo-second-order with pseudo-first-order kinetics, it could be found that pH had an influence on K_{obs}, but not on the nature of As(III) adsorption.

3.3. Effect of initial concentration of heavy metals

Experiments were performed to determine the effect of initial concentration of As(III) on the adsorption capacity of CS-P-NZVI (Table 1). The adsorbed amount was 71.4, 142.9, 214.1 and 260.5 mg/g at 20, 40, 60 and 100 mg/L As(III), respectively (Table 1), indicating that the adsorption capacity to As(III) was raised as an increase in the initial concentration of As(III). Comparison of As (III) or As(V) removal by NZVI was shown in Table 2. The maximum As(III) adsorption capacity was 3.5 mg As(III)/g NZVI and 10 mg As (V)/g NZVI [8]. The As(III) removal capacity of Fe–S coated sand were 41.6 mg As(III)/g Fe–S [28]. The adsorption capacity of NZVI/AC for arsenite and arsenate was 221.9 and 146.3 mg of arsenic per gram of iron, respectively [29]. The higher adsorption capacity for As(III) in the study may be due to the complex cooperation among pumice, chitosan and NZVI. From the result of control experiments (Table 1), it can be seen that higher adsorption capacity is mainly due to the contribution of NZVI particles.

3.4. Effect of the dosage of NZVI

The influence of NZVI dosage (0.28, 0.56, 0.70 and 1.12 g) on the kinetics of adsorption of the As(III) was investigated using 40 mg/L of the As(III) (Table 3). For 0.28–1.12 g NZVI, the K_{obs} were 0.27–0.96 min^{-1} (Table 3). In our experiment, greater than 95% As(III) was adsorbed within 10 min and 99.9% within 60 min, indicating that an initial quicker rate of As(III) removal from aqueous solution took place within 10 min followed by a slower adsorption. This phenomenon was consistent with the results of pseudo-first-order rate of As(V) adsorption by ZVI [30], mercury (II) by pumice-NZVI [14], chromium (VI) by enhanced chitosan/Fe^0-nanoparticles beads [31] and lead (II) adsorption by NZVI [6]. The conclusion could be

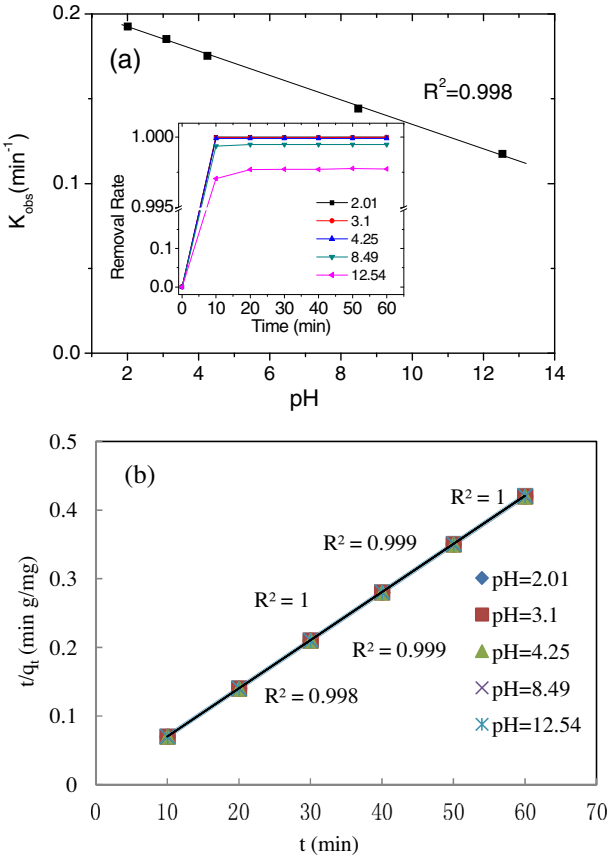

Fig. 2. Kinetics of As(III) adsorption: (a) pseudo-first-order (Inset: the effect of pH on removal rate of As(III)) and (b) pseudo-second-order with respect to the pH values.

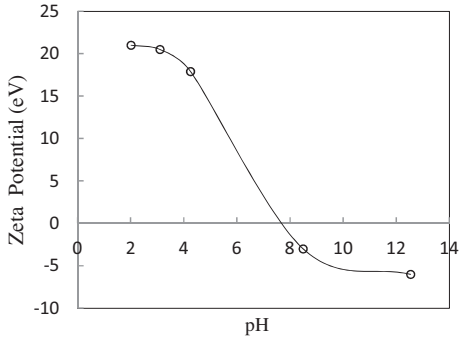

Fig. 3. Zeta-potential as a function of solution pH.

reasonably reached that CS-P-NZVI was effective to remove As(III) from aqueous solution.

3.5. As(III) adsorption isotherms

Adsorption isotherms of As(III) onto CS-P-NZVI were performed at four different temperatures (293–308 K) and initial As(III) concentrations (20–100 mg/L). The Freundlich and Langmuir parameters were obtained by nonlinear least-squares regression analysis [32]. A comparison between Langmuir and Freundlich isotherm constants is presented in Table 4. The Langmuir isotherm model assumed uniform energies and enthalpies of adsorption onto the plane surface [33]. The high correlation coefficients (R^2 > 0.96) suggested that Freundlich isotherm provided a good model of the

Table 1
Effect of initial concentration of As(III) on the adsorbed amount.

Initial concentration of As(III) (mg/L)	Adsorbed amount (mg/g)		
	CS-P-NZVI	CS	CS-P
20	71.4	0.4	1.2
40	142.9	0.6	1.3
60	214.1	0.7	1.5
100	260.5	0.8	1.6

Table 2
Comparison of As(III) or As(V) removal by NZVI.

Adsorbent	Heavy metal	The adsorption capacities
NZVI	As(III)	3.5 mg/g [14]
NZVI colloidal reactive barrier	As(V)	10 mg/g [15]
Fe-S coated sand	As(III)	41.6 mg/g [30]
NZVI/AC	As(III) and As(V)	221.9 and 146.3 mg/g [31]
CS-P-NZVI	As(III)	260.5 mg/g[a]

[a] The result of our study.

Table 3
Effect of NZVI dosages on the kinetics of As(III) adsorption.

NZVI (g)	K_{obs} (min^{-1})	R^2
0.28	0.27	0.99
0.56	0.51	0.95
0.70	0.78	0.97
1.12	0.96	0.96

Table 4
Langmuir and Freundlich isotherm constants at different temperatures. Initial As(III) concentration: 100 mg/L; NZVI: 2.8 g/L; pH: 6.2.

T (K)	Langmuir isotherm parameters			Freundlich isotherm parameters		
	q_m (mg/g)	b	R^2	n	K	R^2
288	242.8	1.488	0.8843	4.832	273.3	0.988
293	218.9	2.030	0.8793	3.523	241.8	0.9763
298	193.0	2.367	0.8950	3.167	216.7	0.9682
303	187.2	3.155	0.8571	2.908	192.2	0.9775

sorption system (Table 4), which was based on heterogeneous adsorption of metal ions. The As(III) adsorption on CS-P-NZVI followed Freundlich better than Langmuir isotherm. Table 4 showed that the exponent n is larger than 1 for adsorption of As(III) on the CS-P-NZVI at different temperatures. The parameter $n > 1$ represents a favorability adsorption condition [34]. The analysis hence suggested that the CS-P-NZVI was heterogeneous in the surface properties. This is in agreement with the results shown in Fig. 1.

The thermodynamic parameters such as enthalpy change (ΔH^0), Gibbs free energy change (ΔG^0) and entropy change (ΔS^0) were also calculated [35] and employed to evaluate the feasibility of the adsorption process. Thermodynamic parameters for adsorption of As(III) onto CS-P-NZVI are shown in Table 5. The negative values of ΔG^0 suggested that the process was spontaneous. The values of ΔG^0 increased with an increase in temperature, indicating that the As(III) adsorption was more favorable at lower temperatures. The phenomenon was also observed by Atkins [36]. The negative values of ΔH^0 suggest that As(III) adsorption by CS-P-NZVI was an exothermic process, which was consistent with previous observation, namely K decreased with an increase in temperature. The positive values of ΔS^0 for all case (Table 5) reflected good affinity of the sorbent for As(III) ions and some structural changes between As(III) (adsorbate) and CS-P-NZVI (adsorbent) [37].

Table 5
Thermodynamic parameters for adsorption of As(III) onto CS-P-NZVI.

ΔH^0 (kJ/mol)	ΔG^0 (kJ/mol)				ΔS^0 (kJ/mol)			
	288 K	293 K	298 K	303 K	288 K	293 K	298 K	303 K
−115.4	−11.6	−9.97	−9.45	−9.10	1.32	1.30	1.29	1.27
−123.3	−11.6	−9.97	−9.45	−9.10	1.38	1.26	1.25	1.23
−128.7	−11.6	−9.97	−9.45	−9.10	0.94	0.93	0.92	0.92
−186.73	−11.6	−9.97	−9.45	−9.10	0.41	0.43	0.45	0.46

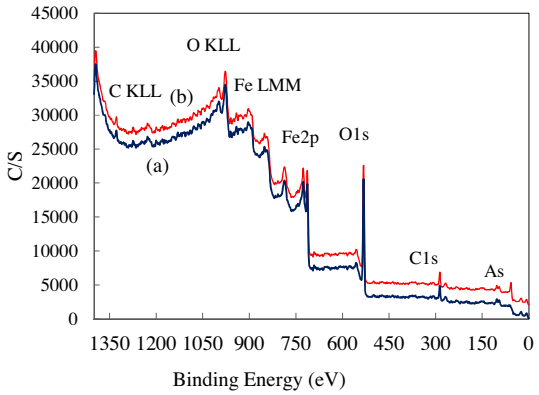

Fig. 4. Typical wide scan XPS spectra for the CS-P-NZVI before (a) and after (b) As (III) adsorption. Initial concentration of As(III): 100 mg/L, NZVI: 0.28 g, pH: 6.12, temperature: 20 °C, time: 1 h.

Table 6
The mass ratio of element on CS-P-NZVI before and after As(III) adsorption.

The mass ratio (%)	Element				
	C1s	O1s	Si2p	Fe2p	As3d
Before	22.6	62.1	4.5	10.8	0
After	22.3	62.0	4.3	10.4	1.0

3.6. The removal mechanisms of As(III)

The results of XPS characterization of CS-P-NZVI before and after As(III) adsorption were shown in Fig. 4. New peak at the binding energy (BE) of 44 eV appeared after As(III) adsorption (Fig. 4 (b)), which was assigned to the photoelectron peak of As. The result of Table 6 showed that before As(III) adsorption, the mass ratio of C, O, Si and Fe was 22.6%, 62.1%, 4.5% and 10.8%, respectively. After As(III) adsorption, the mass ratio of C, O, Si, Fe and As was 22.3%, 62.0%, 4.3%, 10.4% and 1.0% (Table 6), respectively. The phenomena indicated the uptake of As on the surface of CS-P-NZVI.

Table 7
The result of Atomic fluorescence spectrophotometer (AFS) to the valences of As in the treated solution.

Kind of As	Peak height	Peak area	Concentration
As^{3+}	46	4506	3.18 ng/L
As^{5+}	0	0	0

Detailed XPS surveys on the region of As3d and Fe2p were shown in Fig. 5. The only photoelectron peak for As centered at 43.6 eV (Fig. 5(a)), which corresponded to As(III) [27]. The result indicated that As(III) was physically adsorbed without being oxidized on the surface of CS-P-NZVI. However, the different reaction mechanism of As removal was also observed that oxidation occurred in case of As(III) and reduction took place for As(V) only after two months [38]. Due to a high removal rate (more than 99%), the reaction went on for only 1 h in the study, however, oxidation and reduction occurred after more than 60 d as mentioned previously [35]. As NZVI corroded over longer periods, more corrosion products were present for ongoing adsorption of As(III) [8]. Moreover, As(III) near or in contact with the corroding NZVI surface was oxidized to As(V) [39], in turn, inner-sphere As(III) and As(V) surface complexes on iron(III) oxides/hydroxide corrosion products was formed [2,27]. On the other hand, there was little or no reduction in the case of open batch reactors [40]. Other research suggested that the formation of Fe^{2+} and H_2O_2 on the corroding NZVI surface in turn formed OH· radical [41]. However, the introduction of CS disputed the fast corrosion of NZVI, then formation of OH· radical did not happened in 60 min. The finding proved again that NZVI on CS-P-NZVI was better protected against being quickly oxidized by CS. Photoelectron peak at 725.0 eV (Fig. 5(b)) corresponds to the binding energies of $2p_{3/2}$ of oxidized iron [Fe (III)]. The peak at 707.6 eV which is assigned to Fe^0 [42] is also observed in this work. It signified that there was still Fe^0 left and fast oxidation of iron was hindered on the surface of CS-P-NZVI. Furthermore, the phenomenon was also consistent with the result of atomic fluorescence spectrophotometer (AFS) (Table 7), which demonstrated that there was only several ng/L As(III) without As (V) in the treated As solution by CS-P-NZVI.

The results of this study showed that CS-P-NZVI was an efficient material for the treatment of heavy metals and might be used as an effective material for permeable reactive barriers as well as ex situ remediation.

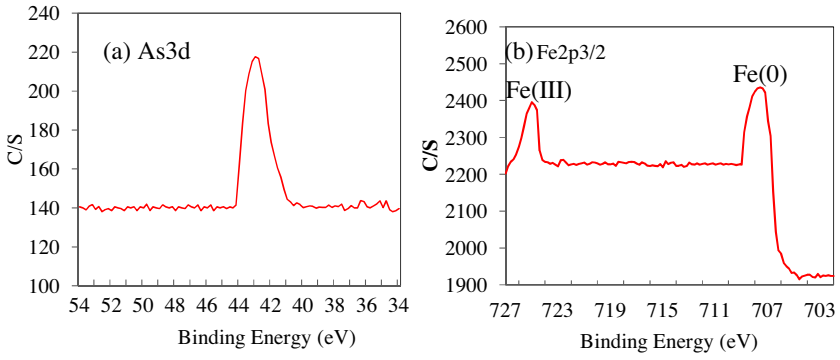

Fig. 5. High-resolution XPS survey of (a) As3d and (b) $Fe2p_{3/2}$ after As(III) adsorption. Initial concentration of As(III): 100 mg/L, NZVI: 0.28 g, pH: 6.12, temperature: 20 °C, time: 1 h.

4. Conclusions

CS-P-NZVI was prepared by loading NZVI onto pumice modified by chitosan and its performance for arsenic(III) removal from wastewater was investigated by batch adsorption experiments. SEM analysis revealed that NZVI on CS-P-NZVI was better protected against aggregating and being oxidized. The results showed that As(III) could be effectively removed by adsorption on NZVI in a very short time at different factors. The removal of As(III) by CS-P-NZVI followed the pseudo-first-order and pseudo-second-order reaction kinetics. The negative values of ΔG^0 and ΔH^0 suggested that As(III) adsorption by CS-P-NZVI was a spontaneous and exothermic process. The positive values of ΔS^0 for all case reflected good affinity of the sorbent for As(III) ions. XPS analyses indicated that As(III) was physically adsorbed without being oxidized on the surface of CS-P-NZVI within 60 min.

Acknowledgments

The authors thank Zhigang Zhang, Qian Wang and Yuntao Shang for their support with analyses. This work was financially supported by the Innovation Team Training Plan of the Tianjin Education Committee (TD12-5037), National Natural Science Foundation of China (21307090) and Tianjin Municipal Natural Science Foundation of China (14JCZDJC41000).

References

[1] V. Mudgal, N. Madaan, A. Mudgal, R.B. Singh, S. Mishra, Effect of toxic metals on human health, Open Nutraceut. J. 3 (2010) 94–99.
[2] B.A. Manning, M. Hunt, C. Amrhein, J.A. Yarmoff, Arsenic (III) and arsenic (V) reactions with zerovalent iron corrosion products, Environ. Sci. Technol. 36 (2002) 5455–5461.
[3] T. Yoshida, H. Yamauchi, G. Fan-Sun, Chronic health effects in people exposed to arsenic *via* the drinking water: dose-response relationships in review, Toxicol. Appl. Pharm. 198 (2004) 243–252.
[4] A. Akcil, C. Erust, S. Ozdemiroglu, V. Fonti, F. Beolchini, A review of approaches and techniques used in aquatic contaminated sediments metal removal and stabilization by chemical and biotechnological processes, J. Cleaner Prod. 86 (2015) 24–36.
[5] S. Dixit, J.G. Hering, Comparison of arsenic (V) and arsenic (III) sorption onto iron oxide minerals: implications for arsenic mobility, Environ. Sci. Technol. 37 (2003) 4182–4189.
[6] S.M. Ponder, J.C. Darab, T.E. Mallouk, Remediation of Cr (VI) and Pb (II) aqueous solutions using supported, nanoscale zerovalent iron, Environ. Sci. Technol. 34 (2000) 2564–2569.
[7] W.X. Zhang, Nano scale iron particles for environmental remediation: an overview, J. Nanopart. Res. 5 (2003) 323–332.
[8] S.R. Kanel, B. Manning, L. Charlet, H. Choi, Removal of arsenic (III) from groundwater by nanoscale zero-valent iron, Environ. Sci. Technol. 39 (2005) 1291–1298.
[9] F. He, D.Y. Zhao, Preparation and characterization of a new class of starch-stabilized bimetallic nanoparticles for degradation of chlorinated hydrocarbons in water, Environ. Sci. Technol. 39 (2005) 3314–3320.
[10] S.R. Kanel, H. Choi, Transport characteristics of surface-modified nanoscale zero-valent iron in porous media, Water Sci. Technol. 55 (1–2) (2007) 157–162.
[11] B. Geng, Z.H. Jin, T.L. Li, X.H. Qi, Kinetics of hexavalent chromium removal from water by chitosan-Fe^0 nanoparticles, Chemosphere 75 (2009) 825–830.
[12] F. He, M. Zhang, T. Qian, D. Zhao, Transport of carboxymethyl cellulose stabilized iron nanoparticles in porous media: column experiments and modeling, J. Colloid Interface Sci. 334 (1) (2009) 96–102.
[13] A. Tiraferri, K.L. Chen, R. Sethi, M. Elimelech, Reduced aggregation and sedimentation of zero-valent iron nanoparticles in the presence of guar gum, J. Colloid Interface Sci. 324 (2008) 71–79.
[14] T. Liu, Z.L. Wang, Y. Sun, Manipulating the morphology of nanoscale zero-valent iron on pumice for removal of heavy metals from wastewater, Chem. Eng. J. 263 (2015) 55–61.
[15] Z. Li, H.K. Jones, P.P. Zhang, R.S. Bowman, Chromate transport through columns packed with surfactant-modified zeolite/zero valent iron pellets, Chemosphere 68 (2007) 1861–1866.
[16] L.N. Shi, X. Zhang, Z.L. Chen, Removal of chromium (VI) from wastewater using bentonite-supported nanoscale zero-velant iron, Water Res. 45 (2011) 886–892.
[17] Y.S. Ho, D.A.J. Wase, C.F. Forster, Batch nickel removal from aqueous solution by sphagnum moss peat, Water Res. 29 (5) (1995) 1327–1332.
[18] A.R. Iftikhar, H.N. Bhatti, M.A. Hanif, R. Nadeem, Kinetic and thermodynamic aspects of Cu (II) and Cr (III) removal from aqueous solutions using rose waste biomass, J. Hazard. Mater. 161 (2009) 941–947.
[19] X.Q. Li, J.S. Cao, W.X. Zhang, Stoichiometry of Cr (VI) immobilization using nanoscale zerovalent iron (nZVI): a study with high-resolution X-ray photoelectron spectroscopy (HR-XPS), Ind. Eng. Chem. Res. 47 (2008) 2131–2139.
[20] M.M. Ramos-Tejada, A. Ontiveros, J.L. Viota, J.D.G. Duran, Interfacial and rheological properties of humic acid/hematite suspensions, J. Colloid Interface Sci. 268 (2003) 85–95.
[21] T. Liu, L. Zhao, D. Sun, X. Tan, Entrapment of nanoscale zero-valent iron in chitosan beads for hexavalent chromium removal from wastewater, J. Hazard. Mater. 184 (2010) 724–730.
[22] J. Yin, M.P. Rainka, X.X. Zhang, S.L. Buchwald, A highly active Suzuki catalyst for the synthesis of sterically hindered biaryls: novel ligand coordination, J. Am. Chem. Soc. 124 (7) (2002) 1162–1163.
[23] T. Kurahashi, K. Oda, M. Sugimoto, T. Ogura, H. Fujii, Trigonal-bipyramidal geometry induced by an external water ligand in a sterically hindered iron salen complex, related to the active site of protocatechuate 3,4-dioxygenase, Inorg. Chem. 45 (2006) 7709–7721.
[24] B.C. Hamann, J.F. Hartwig, Sterically hindered chelating alkyl phosphines provide large rate accelerations in palladium-catalyzed amination of aryl iodides, bromides, and chlorides, and the first amination of aryl tosylates, J. Am. Chem. Soc. 120 (1998) 7369–7370.
[25] T.Y. Liu, L. Zhao, X. Tan, S.J. Liu, J.J. Li, Y. Qi, G.Z. Mao, Effects of physicochemical factors on Cr (VI) removal from leachate by zero-valent iron and a-Fe_2O_3 nanoparticles, Water Sci. Technol. 61 (2010) 2759–2767.
[26] B.A. Manning, S.E. Fendorf, S. Goldberg, Surface structures and stability of arsenic (III) on goethite: spectroscopic evidence for inner-sphere complexes, Environ. Sci. Technol. 32 (1998) 2383–2388.
[27] J. Farrell, J. Wang, P. O'Day, M. Coklin, Electrochemical and spectroscopic study of arsenate removal from water using zerovalent iron media, Environ. Sci. Technol. 35 (2001) 2026–2032.
[28] Y.S. Han, T.J. Gallegos, A.H. Demond, K.F. Hayes, FeS-coated sand for removal of arsenic (III) under anaerobic conditions in permeable reactive barriers, Water Res. 45 (2011) 593–604.
[29] H. Zhu, Y. Jia, X. Wu, H. Wang, Removal of arsenic from water by supported nano zero-valent iron on activated carbon, J. Hazard. Mater. 172 (2009) 1591–1596.
[30] N. Melitas, J. Wang, M. Conklin, P. O'Day, J. Farrell, Understanding soluble arsenate removal kinetics by zerovalent iron media, Environ. Sci. Technol. 36 (2002) 2074–2081.
[31] T. Liu, Z.L. Wang, L. Zhao, X. Yang, Enhanced chitosan/Fe^0-nanoparticles beads for hexavalent chromium removal from wastewater, Chem. Eng. J. 189–190 (2012) 196–202.
[32] Z. Reddad, C. Gerente, Y. Andres, P.L. Cloirec, Adsorption of several metal ions onto a low-cost biosorbent: kinetic and equilibrium studies, Environ. Sci. Technol. 36 (2002) 2067–2073.
[33] N.S. Kumar, M. Suguna, V. Subbaiah, A.S. Reddy, N.P. Kumar, A. Krishnaiah, Adsorption of phenolic compounds from aqueous solutions onto chitosan-coated perlite beads as biosorbent, Ind. Eng. Chem. Res. 49 (2010) 9238–9247.
[34] T.Y. Guo, Y.Q. Xia, G.J. Hao, M.D. Song, B.H. Zhang, Adsorptive separation of hemoglobin by molecularly imprinted chitosan beads, Biomaterials 25 (2004) 5905–5912.
[35] M. Ajmal, A.H. Khan, S. Ahmad, A. Ahmad, Role of sawdust in the removal of copper (II) from industrial wastes, Water Res. 32 (1998) 3085–3091.
[36] P.W. Atkins, Physical Chemistry, fifth ed., W. H. Freeman and Company, New York, 1994.
[37] V.K. Gupta, Equilibrium uptake, sorption dynamics, process development and column operations for the removal of copper and nickel from aqueous solution and wastewater using activated slag, a low-cost adsorbent, Ind. Eng. Chem. Res. 37 (1998) 192–202.
[38] C. Su, R.W. Puls, Arsenate and arsenite removal by zerovalent iron: kinetics, redox transformation, and implications for in situ groundwater remediation, Environ. Sci. Technol. 35 (2001) 1487–1492.
[39] S.E. Fendorf, M.J. Eick, P. Grossl, D.L. Sparks, Arsenate and chromate retention mechanisms on goethite. 1. surface structure, Environ. Sci. Technol. 31 (2) (1997) 315–320.
[40] N. Melitas, M. Conklin, J. Farrell, Electrochemical study of arsenate and water reduction of iron media used for arsenic removal from potable water, Environ. Sci. Technol. 36 (2002) 3188–3193.
[41] S.H. Joo, A.J. Feitz, T.D. Waite, Oxidative degradation of the carbothioate herbicide, molinate, using nanoscale zero-valent iron, Environ. Sci. Technol. 38 (2004) 2242–2247.
[42] S. Chatterjee, D.S. Lee, M.W. Lee, S.H. Woo, Nitrate removal from aqueous solutions by cross-linked chitosan beads conditioned with sodium bisulfate, J. Hazard. Mater. 166 (1) (2009) 508–513.